BIOCHEMISTRY
including biophysical chemistry & molecular biology

Article

pubs.acs.org/biochemistry

Open Access on 07/16/2015

Structural and Functional Characterization of a Cytochrome P450 2B4 F429H Mutant with an Axial Thiolate−Histidine Hydrogen Bond

Yuting Yang,[†] Haoming Zhang,[†] Dandamudi Usharani,[§] Weishu Bu,[†] Sangchoul Im,[†] Michael Tarasev,[†] Freeborn Rwere,[†] Naw May Pearl,[†] Jennifer Meagher,[‡] Cuthbert Sun,[†] Jeanne Stuckey,[‡] Sason Shaik,[§] and Lucy Waskell*,[†]

[†]Department of Anesthesiology, University of Michigan and VA Medical Center, 2215 Fuller Road, Building 31, Room 225, Ann Arbor, Michigan 48105, United States

[‡]Life Science Institute, University of Michigan, 210 Washtenaw Avenue, Ann Arbor, Michigan 48109, United States

[§]Institute of Chemistry and Lise Meitner-Minerva Center for Computational Quantum Chemistry, Hebrew University of Jerusalem, 91904 Jerusalem, Israel

Supporting Information

ABSTRACT: The structural basis of the regulation of microsomal cytochrome P450 (P450) activity was investigated by mutating the highly conserved heme binding motif residue, Phe429, on the proximal side of cytochrome P450 2B4 to a histidine. Spectroscopic, pre-steady-state and steady-state kinetic, thermodynamic, theoretical, and structural studies of the mutant demonstrate that formation of an H-bond between His429 and the unbonded electron pair of the Cys436 axial thiolate significantly alters the properties of the enzyme. The mutant lost >90% of its activity; its redox potential was increased by 87 mV, and the half-life of the oxyferrous mutant was increased ∼37-fold. Single-crystal electronic absorption and resonance Raman spectroscopy demonstrated that the mutant was reduced by a small dose of X-ray photons. The structure revealed that the δN atom of His429 forms an H-bond with the axial Cys436 thiolate whereas the εN atom forms an H-bond with the solvent and the side chain of Gln357. The amide of Gly438 forms the only other H-bond to the tetrahedral thiolate. Theoretical quantification of the histidine−thiolate interaction demonstrates a significant electron withdrawing effect on the heme iron. Comparisons of structures of class I−IV P450s demonstrate that either a phenylalanine or tryptophan is often found at the location corresponding to Phe429. Depending on the structure of the distal pocket heme, the residue at this location may or may not regulate the thermodynamic properties of the P450. Regardless, this residue appears to protect the thiolate from solvent, oxidation, protonations, and other deleterious reactions.

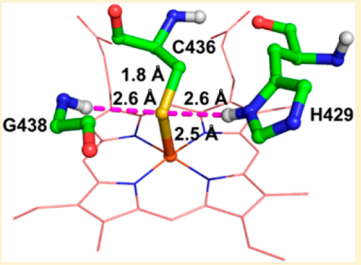

The P450s make up a ubiquitous superfamily of mixed-function oxygenases that catalyze a variety of chemical reactions and play vital roles in important biological processes.[1−6] One of the most highly conserved residues of the P450s is the phenylalanine in the heme binding motif (FXXGXR/HXCXG), located on the proximal side of the heme where its redox partners bind.[7,8] The phenylalanine is in van der Waals (vdw) contact with the heme and the axial Cys436 thiolate. As a result, it is strategically positioned to influence P450 activity by modulating the electron donating ability of the thiolate. While the properties of most of the corresponding phenylalanine to histidine mutants of class I and II P450s indicate a key role for the phenylalanine in the regulation of catalytic activity, there are intriguing exceptions (CYP121 and $P450_{cin}$).[7,9−20] In some class III P450s that are isomerases rather than monooxygenases, the phenylalanine is replaced with a tryptophan.[21−23] Nitric oxide reductase, a class IV enzyme, retains the phenylalanine.[24] These observations raise the question of the function of the conserved phenylalanine and the molecular and atomic level mechanism by which residues in the heme binding motif exert their delicately balanced effects in a particular P450.[25] A related consideration is if phenylalanine is not important for activity and thermodynamic properties, then what other residues control these parameters?

In an effort to gain insight into the structural basis and regulation of catalysis in microsomal P450s in particular and P450s in general, Phe429 in CYP2B4 has been mutated to histidine and the mutant protein has been characterized.[26−29] One of the key experimental and theoretical findings was that a unique H-bond between the histidine and the axial cysteine, which alters electron density on the axial thiolate, adversely affects enzymatic activity. This suggests that Phe429, by virtue of its steric bulk and relative chemical inertness, not only protects the protein from deleterious interactions but also may be modified to generate desirable enzymatic activities. Our findings and comparison to other heme proteins reveal that P450s employ a variety of residues on both the proximal and

Received: March 28, 2014
Revised: July 15, 2014
Published: July 16, 2014

distal surfaces to regulate the versatility of the catalytic repertoire and mechanisms of P450s.

MATERIALS

Yeast extract, tryptone, and glycerol were purchased from Fisher Scientific. Dilauroylphosphatidylcholine (DLPC) was purchased from Doosan Serdary Research laboratories. Sodium cholate (>99% pure) was obtained from Anatrace. Isopropyl β-D-thiogalactopyranoside (IPTG), carbenicillin (disodium salt), and δ-aminolevulinic acid were from Research Products International Corp. DE52 medium (preswollen diethylaminoethylcellulose) was from Whatman. Bio-Beads SM-2 and hydroxyapatite resins were from Bio-Rad. Dithiothreitol, Tergitol NP-10, nonaethylene glycol monododecyl ether (Brij), benzphetamine, Cymal-5, Reactive Red 120 type 300-CL, Octyl Sepharose CL-4B, 2,6-di-*tert*-butyl-4-methylphenol butylated hydroxytoluene (BHT), sodium borohydride, sodium dithionite, Trizma base, and lysozyme were from Sigma-Aldrich. DNase and the protease inhibitor cocktail were purchased from Roche Diagnostics Corp. (Indianapolis, IN). 4-(4-Chlorophenyl)imidazole (4-CPI) was purchased from Oakwood Products, Inc. The 50% PEG 3350 solution, 50% PEG 8000 solution, 10% (w/v) Anapoe-X-114 solution, 1 M magnesium acetate solution, 1 M sodium cacodylate solution, and 1 M HCl solution were purchased from Hampton Research.

EXPERIMENTAL PROCEDURES

Overview of the Purification of Truncated F429H. Truncated CYP2B4 F429H refers to a CYP2B4 in which residues 3−21 were deleted and the following mutations were introduced: G22K, H23K, P24T, K25S, A26S, H27K, and R29K. An H226Y mutation was made and a four-histidine tag added at the carboxyl terminus as described previously.[30] The cell pellet was prepared by sonication, solubilization, and ultracentrifugation before being loaded on a series of chromatography columns, including DE52, Reactive Red, Octyl Sepharose, and hydroxyapatite columns, as previously described.[31] Because the F429H mutant protein is more susceptible to inactivation to cyt P420, butylated hydroxyl toluene (BHT) was added to all buffers (to scavenge free radicals formed by the ether-containing detergent). The pure protein was concentrated to ∼1 mM using a 50000 molecular weight cutoff VivaSpin 20 and immediately used for crystallization experiments. The details of the purification are provided in the Supporting Information.

Crystallization, Data Collection, Structure Determination, and Refinement. Crystals of truncated CYP2B4 F429H were obtained using the hanging or sitting drop vapor diffusion method by mixing 2 μL of the previously described protein solution, 2 μL of the reservoir solution, and 0.4 μL [10% (w/v)] of Anapoe X-114 to facilitate crystallization. The crystallization trays were both set up and incubated at 4 °C. The crystals were transferred to a cryoprotectant, flash-frozen, and stored in liquid nitrogen prior to data collection.

The data set was processed using HKL2000 0.98.703g.[32] The structure was determined using the molecular replacement program Phaser 2.1.4[33] in the CCP4 6.1.13 suite.[34] The model was refined using AutoBuster[35] and manually rebuilt in COOT 0.6.2[36] and O 10.0.3.[37] The ligand CIF files for heme and 4-CPI were generated using GRADE 1.1.1.[38] Structure validations were conducted in MolProbity 3.17.[39] The structure scored at the 100% percentile for quality among structures of similar resolution, based on Ramachandran, rotamer, C_β deviation, bond length, or angle analysis. Details of the crystallization procedure are provided in the Supporting Information.

Activity of F429H CYP2B4. The activity of mutant full length CYP2B4 was determined in a purified reconstituted system by measuring the amount of formaldehyde formed by N-demethylation of benzphetamine (BP) using Nash's reagent as previously described.[40] Wild type P450 and P450 reductase were purified as described previously.[31,41]

Determination of the Affinity (K_s) of CYP2B4 for Substrates in the Presence of P450 Reductase and Cyt b_5 and the Apparent K_m between the P450 and P450 Reductase. The following biochemical experiments were performed with the full length wild type (WT) and the CYP2B4 F429H as previously described[40] and with full length reductase and cyt b_5 purified as previously described.[40,41] The dissociation constant K_s between the substrate benzphetamine and the P450s was determined by measuring the type I spectral change that occurs when benzphetamine binds to P450.[42] In a typical experiment, P450 [5−10 μM in 15% glycerol in 50 mM KPO_4 buffer (pH 7.4)] was placed in the temperature-controlled sample and the reference cuvettes, maintained at either 15 or 30 °C. After 10 min, a stable baseline was recorded. An aliquot of a benzphetamine-containing stock solution was then added to the sample cuvette, and an equal volume of buffer A [0.1 M KPO_4 buffer (pH 7.4) and 15% glycerol] was added to the reference cuvette. The difference spectrum was recorded 5 min after the addition of benzphetamine. The concentration of benzphetamine varied from 0.04 to 1 mM. The absolute absorbance change from 382 to 420 nm ($\Delta A_{382-420}$) was plotted versus the concentration of benzphetamine. The absorbance changes were corrected for dilution. An isosbestic point was observed at 405 nm in the absolute spectra upon conversion from low to high spin.

The apparent K_m of the CYP2B4−P450 reductase complex was determined by measuring the rate of N-demethylation of benzphetamine at various reductase concentrations as previously described.[40] WT CYP2B4 (0.16 nmol) or 0.4 nmol of mutant CYP2B4 F429H was mixed with a 0.25−5-fold molar excess of P450 reductase and a 200-fold molar excess of DLPC in 50 mM potassium phosphate buffer (pH 7.4) and incubated for 1 h at room temperature. The solution was then diluted to 0.8 mL with 50 mM potassium phosphate buffer (pH 7.4) containing 1 mM benzphetamine (final concentration of 0.2 μM for WT 2B4 and 0.5 μM for mutant F429H). The reaction was initiated by the addition of NADPH (final concentration of 300 μM). V_{max} and K_m were determined by fitting the rate of formaldehyde formation at each reductase concentration as described previously.[40]

Determination of the Midpoint Redox Potential (E_m) of CYP2B4 F429H by the Dye Equilibrium Method. The midpoint redox potentials, E_m, of the full length WT and CYP2B4 F429H were determined at 20 °C in buffer A [0.1 M potassium phosphate and 15% glycerol (pH 7.4)] as described previously.[43] Benzyl viologen (E_m = −341 mV) and phenosafranin (E_m = −244 mV) were used as the redox dyes because the E_m values of these two dyes are similar to those of the wild type and P450 F429H. We note that the absolute values of the E_m of benzyl viologen and phenosafranin vary in the literature with a range of values from −0.31 to 0.35 V for benzyl viologen and from −0.244 to 0.252 V for phenosafranin

dx.doi.org/10.1021/bi5003794 | *Biochemistry* 2014, 53, 5080−5091

at pH 7 and 20 °C.[43,44] This variation will dictate the absolute E_m value of P450s determined in this work.

The experiments were performed in an anaerobic tonometer. All glassware and solutions were deoxygenated overnight in an anaerobic glovebox (Belle Technology) with an oxygen content of ∼1 ppm. In a typical experiment, 1 mL of an 8 μM solution of CYP2B4 was incubated overnight in buffer A at 4 °C in the presence of 0.38 mM dilauroyl-L-3-phosphatidylcholine (DLPC) to remove oxygen and prevent aggregation in the subsequent titration with sodium dithionite. Prior to the titration with dithionite, the dye was added to the P450 sample at a final concentration of 16 μM. In the case of studying the effect of substrate on E_m, benzphetamine was included in the P450 samples at a final concentration of 1 mM. A standardized solution of sodium dithionite (∼80 μM) was added in 2 μL increments to the mixture of P450 and the mediator. The spectra were recorded on a Cary 300 spectrophotometer, prior to the addition of dithionite and following each addition of each aliquot of dithionite once the spectral changes had stabilized. The spectra recorded at the start and end of the titration represent fully oxidized and fully reduced P450, respectively. The ratio of the oxidized P450 versus the reduced P450 ($P450_{Ox}/P450_{Re}$) was calculated from the absorbance at 450 nm in the presence of benzyl viologen and at 405 nm in the presence of phenosafranin. Benzyl viologen shows minimal absorbance changes at 450 nm when it is reduced, while phenosafranin has an isosbestic point at 405 nm. The ratio of the oxidized to the reduced dye (dye_{Ox}/dye_{Re}) was calculated from the absorbance at 730 nm for benzyl viologen and 520 nm for phenosafranin. The E_m of P450 was calculated according to the Nerst equation: $E = E_m + RT/F \ln(P450_{Ox}/P450_{Re})$, where F, R, and T are the Faraday constant (9.65×10^4 C mol^{-1}), gas constant (8.31 J K^{-1} mol^{-1}), and temperature (kelvin), respectively.

Determination of the Rate Constant for the Transfer of an Electron from P450 Reductase to Ferric CYP2B4. The rate of transfer of an electron from full length P450 reductase to ferric P450 was determined as previously described.[45] A solution containing ∼5 μM P450 and ∼5 μM P450 reductase was incubated in an anaerobic glovebox (Belle Technology) at 4 °C overnight in buffer A containing 0.3 mM dilauroyl-L-3-phosphatidylcholine (DLPC) and 1 mM benzphetamine to preform a P450−P450 reductase complex in a stopped-flow spectrophotometer (model SF-61 DX2, Hi-Tech), housed in a glovebox. The second syringe was loaded with CO-saturated buffer A that contained 0.3 mM NADPH and 1 mM benzphetamine. The rate of reduction of P450 by P450 reductase was monitored at 450 nm.[46] The rate of the first electron transfer was determined by fitting the absorbance traces at 450 nm with multiple exponentials using KinetAsyst software (Hi-Tech).

Determination of the Kinetics of the Autoxidation of Oxyferrous CYP2B4 F429H. The kinetics of the autoxidation of full length P450s were determined as previously described.[47] Briefly, the P450 in 15% glycerol and 0.1 M potassium phosphate buffer (pH 7.4) was reduced with a standardized solution of sodium dithionite in an anaerobic tonometer. The reduced protein was introduced into one syringe of the stopped-flow spectrophotometer (Hi-Tech SF61DX2 in a glovebox) and rapidly mixed with an air-saturated solution ($[O_2] \cong 0.32$ mM at 15 °C) of buffer. The experiments were performed at 15 °C in the presence of 5−10 μM P450 in buffer A and 1 mM benzphetamine with a Hi-Tech stopped-flow 61 DX2 spectrophotometer housed in a glovebox. The kinetics of autoxidation were monitored at 438 nm after the sample had been rapidly mixed with an air-saturated buffer solution ($[O_2] \cong 0.32$ mM). Rate constants and amplitudes were obtained by fitting the kinetic traces at 438 nm with multiple exponentials using KinetAsyst software (Hi-Tech).

Theoretical Calculations. The details of the setup and procedures for the QM/MM calculations are provided in the Supporting Information.

RESULTS

Steady-State Activity of CYP2B4 F429H. The F429H mutant exhibits a significant decrease in activity (N-demethylation of BP), retaining only 3.6% [V_{max} = 1.60 ± 0.05 nmol of product min^{-1} (nmol of 450)$^{-1}$] of the wild type activity [V_{max} = 49 ± 5 nmol of product min^{-1} (nmol of 450)$^{-1}$]. The apparent K_m (0.067 ± 0.004 μM) of P450 reductase for the WT and F429H mutant is similar, indicating that the low activity of the mutant is not caused by a decreased affinity for the reductase. The activity of both proteins is coupled to the same extent, ∼50% (50% of NADPH utilized for product formation). Mutation of the homologous phenylalanine to histidine in $P450_{cam}$ and BM3 resulted in an ∼85% loss of activity.[9,12] The significant loss of activity in three different model P450s (including class I and class II proteins with ferredoxin and flavin redox partners, respectively) in which the highly conserved phenylalanine at the beginning of the β-bulge has been mutated to histidine attests to the key role this residue plays in P450 catalysis.

UV−Visible Spectra of CYP2B4 F429H. In the absence of substrate, both the wild type and F429H mutant have a spectrum of a low-spin ferric heme with a Soret peak at 416 and broad α and β bands at 571 and 534 ± 3 nm, respectively. The absorption maximum of the F429H ferrous−CO complex is blue-shifted from 450 nm in the wild type to 446 nm in the mutant. These changes in the UV−visible spectrum of the mutant are consistent with the changes in axial ligand bonding that alter the energy levels between the sulfur π and the porphyrin π* orbitals.[48] In P450s, with the more electron-donating selenocysteine rather than the sulfur-containing cysteine as an axial ligand, the maxima of the Fe−CO complex and high-spin ferric protein are red-shifted compared to those of the wild type proteins.[25,49]

Affinity of CYP2B4 F429H for Substrates in the Presence and Absence of P450 Reductase and Cytochrome b_5 (cyt b_5). Addition of benzphetamine to wild type P450 results in a change in spin state that causes a type I spectral change (a decrease in absorbance at 416 nm and an increase at 385 nm and a charge transfer band at 650 nm). This spectral change is generally considered to reflect the binding of substrate, and its measurement is known as K_s. However, because substrates can bind without displacing the heme iron water ligand, it is actually a surrogate measure of the affinity of substrates for P450s denoted as K_s. Surprisingly, at 15 °C, the addition of benzphetamine to F429H caused an only marginal spectral change (Table 1), which illustrates that the mutant exhibits a K_s of 0.9 ± 0.2 mM while the wild type binds with a K_s of 0.25 ± 0.01 mM. At 30 °C, the binding of benzphetamine to both WT and F429H is enhanced by a similar amount, as suggested by the decreased K_s values. Nonetheless, the mutant continued to show an apparent 5-fold decreased affinity for benzphetamine. A second substrate, butylated hydroxytoluene, also caused a change in the spin state

dx.doi.org/10.1021/bi5003794 | Biochemistry 2014, 53, 5080−5091

Table 1. Dissociation Constants of Benzphetamine for the Wild Type and P450 F429H

P450	reductase	cyt b_5	T (°C)	K_s (mM)
WT	−	−	15	0.25 ± 0.007
	−	+	15	0.058 ± 0.006
	+	−	15	0.22 ± 0.01
	−	−	30	0.08 ± 0.02
F429H	−	−	15	0.90 ± 0.20
	−	+	15	0.15 ± 0.06
	+	−	15	0.83 ± 0.22
	−	−	30	0.39 ± 0.08

of the mutant smaller than that of the wild type [K_s of 0.31 ± 0.14 μM for WT and K_s of 1.82 ± 0.24 μM for F429H at 25 °C in 100 mM KP_i (pH 7.4), 15% glycerol, and 0.3 M NaCl]. The question of whether the stability of the low-spin form in the presence of the substrate benzphetamine is a consequence of electronic or structural factors or both remains unanswered at this time. It is not possible to determine whether (1) the substrate does not bind or (2) it binds but does not displace the axial water. A third possibility is that one of the hydroxyl groups on butylated hydroxytoluene binds to the heme iron and displaces the axial water. The crystal structure of the F429H mutant protein does not suggest a structural explanation. An electronic attribution is also somewhat problematic because P450s with a more electron-donating selenocysteine rather than the sulfur-containing cysteine as an axial ligand also stabilize the low-spin ferric form.[25,49] The K_s for benzphetamine remains virtually unchanged for both proteins in the presence and absence of P450 reductase. In contrast, cyt b_5 enhances the binding of benzphetamine to both proteins by ∼5−6-fold, indicating that the mutant protein is responsive to cyt b_5 (Table 1).[50]

Midpoint Redox Potential (E_m) of CYP2B4 F429H. The midpoint redox potentials, E_m, were determined in the absence and presence of 1 mM benzphetamine at 20 °C. To ensure that the redox dyes were not interfering with measurements of E_m, we investigated the binding of the redox mediator dyes, benzyl viologen and phenosafranin, to P450 and determined the E_m at three different P450/dye molar ratios. The addition of the redox dyes to P450 did not cause any spectral change, and the E_m was independent of the protein/dye ratio (data not shown). As presented in Table 2 and Figure 1, the E_m of WT is −332 ± 8 mV in the absence of benzphetamine, which is in agreement with the E_m values of −330 to −300 mV published in the literature.[43] In clear contrast, the E_m of F429H is −245 ± 6 mV in the absence of benzphetamine, which is an increase of 87 mV compared to that of the WT. For the WT and F429H P450s examined in this study, the binding of benzphetamine led to increases in E_m of 88 and 15 mV, respectively, indicating that the binding of benzphetamine to the active site modulates the redox potential of CYP2B4, presumably by altering the polarity of the active site.

Table 2. Midpoint Redox Potentials of CYP2B4 at 20 °C and pH 7.4

	redox potential E_m (mV)	
P450	without BP	with BP
WT	−332 ± 8	−244 ± 7
F429H	−245 ± 6	−230 ± 8

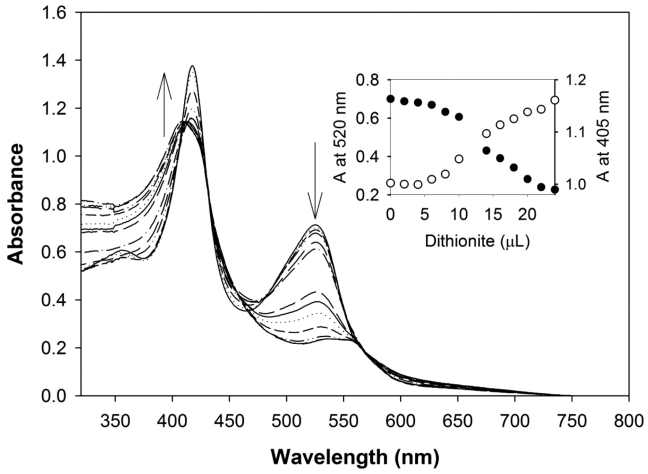

Figure 1. Spectral changes observed during the course of determining the redox potential of F429H in the presence of phenosafranin. A solution containing 8 μM ferric F429H and 16 μM phenosafranin was reduced with 2 μL increments of a standardized dithionite solution. Reduction of F429H was monitored at 405 nm (○), an isosbestic point for phenosafranin, whose reduction was followed by 520 nm (●). The arrows indicate the direction of the absorbance changes during reduction. The potential was calculated as described in Experimental Procedures.

Rate of Transfer of an Electron from P450 Reductase to Ferric F429H. To investigate the effect of an 87 mV more positive redox potential on the reduction of ferric F429H by P450 reductase, the kinetics of transfer of an electron to the ferric mutant enzyme were measured in the presence of substrate and CO. The kinetics of reduction of the ferric WT and F429H mutant proteins are biphasic (Figure 2 and Table 3). As expected, the high-potential F429H protein is reduced more rapidly than the wild type.

Stability of Oxyferrous CYP2B4 F429H. The kinetics of autoxidation of F429H were monophasic (k = 0.12 ± 0.02 min^{-1}) at 15 °C in the presence of 1 mM benzphetamine. Oxyferrous F429H is relatively stable with a half-life of ∼5 min (Figure 3). In contrast, wild type CYP2B4 autoxidized much more rapidly with biphasic rate constants (amplitudes) of 0.13

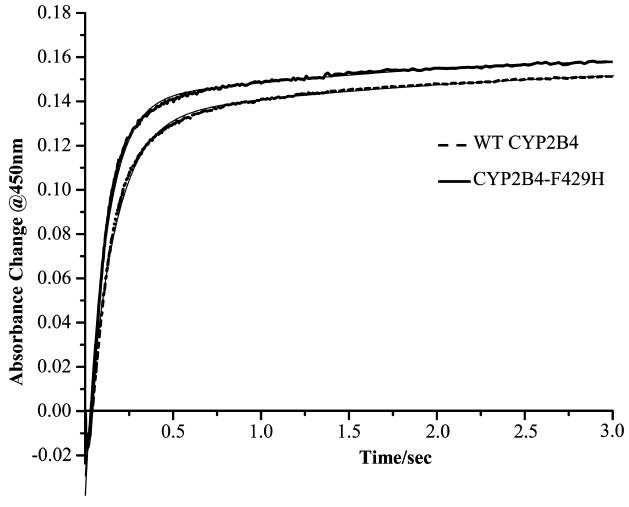

Figure 2. Kinetics of transfer of an electron from P450 reductase to ferric F429H: (---) WT and (—) F429H. The experiments were performed as described in Experimental Procedures.

dx.doi.org/10.1021/bi5003794 | Biochemistry 2014, 53, 5080−5091

Table 3. Rate Constants and Relative Amplitudes of Transfer of an Electron from P450 Reductase to Ferric P450s at 15 °C[a]

P450	phase I (s^{-1}) (%)	phase II (s^{-1}) (%)
WT	4.5 ± 0.1 (85.4 ± 0.2)	0.11 ± 0.01 (14.6 ± 0.2)
F429H	6.1 ± 0.1 (86.4 ± 0.1)	0.14 ± 0.001 (13.6 ± 0.1)

[a]Values in parentheses are amplitudes in percentage.

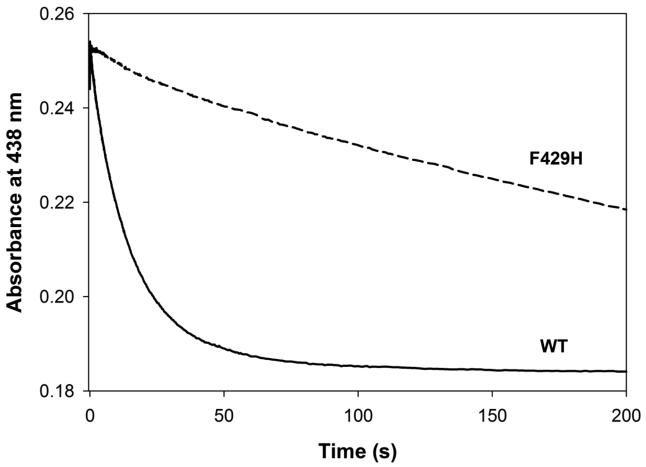

Figure 3. Kinetics of autoxidation of oxyferrous F429H. The experiments were performed as described in Experimental Procedures.

± 0.04 s^{-1} (40 ± 4%) and 0.048 ± 0.004 s^{-1} (60 ± 7%), respectively, and an ~7.6 s half-life.[47] The enhanced stability of the distal ligand–heme bond demonstrates the ability of the residue at the conserved phenylalanine position to regulate the electronic properties of the heme iron.[27,29] Less electronegativity on the heme iron results in a tighter heme–trans ligand interaction.[51] In model porphyrins, H-bonds to the axial thiolate have also been shown to influence the reactivity of the heme iron.[52]

Reduction of CYP2B4 F429H/4-(4-Chlorophenyl) Imidazole (4-CPI) in the X-ray Beam. Previous experiments have shown that metalloproteins and heme proteins in particular are frequently reduced by solvated electrons generated by X-ray photons at cryogenic temperatures of 100 K, the temperature at which crystals are routinely irradiated.[53−57] This information prompted us to investigate whether CYP2B4 F429H/4-CPI was reduced during the course of irradiation of the crystal.

The spectra of crystals of CYP2B4 F429H bound to 4-CPI were recorded before and after irradiation. Figure 4A demonstrates a partial shift in the Soret peak from 415 nm in the oxidized protein to 450 nm after only a single 1 s exposure to 1.075 Å irradiation. Using RADDOSE, version 3, it was estimated that 0.17 MGy had been absorbed by the crystal after 1 s, which is significantly smaller than the radiation dose limit of 30 MGy.[57] This red shift of the Soret is slightly different from that observed when the mutant protein is reduced in solution by dithionite. In solution, the maximal absorbance change is from 422 nm for the ferric protein to 444 nm for the reduced protein. This minor discrepancy between the crystal and solution spectra of proteins has been observed in other heme proteins and has been attributed to the anisotropic properties of crystals.[54] Reduction was also confirmed by the emergence of a sharp peak in absorbance at 566 nm (569 nm in solution) after irradiation of the crystal. The mutant protein continued to be reduced throughout the irradiation with significant degradation of the intensity of the reflections.

Resonance Raman spectra also documented the redox state of the crystallized protein using the 532 nm laser available at Brookhaven National Laboratory (Upton, NY). The 532 nm laser excites and is in resonance primarily with the α and β band transitions between 530 and 580 nm. Nevertheless, it was possible to excite with low intensity the "oxidation-state" marker band, ν_4, appearing at 1373 cm^{-1} for the ferric F429H/4-CPI species[15] (Figure 4B). Upon exposure to X-rays, this "oxidation-state" marker band shifted by 8 cm^{-1} to a lower

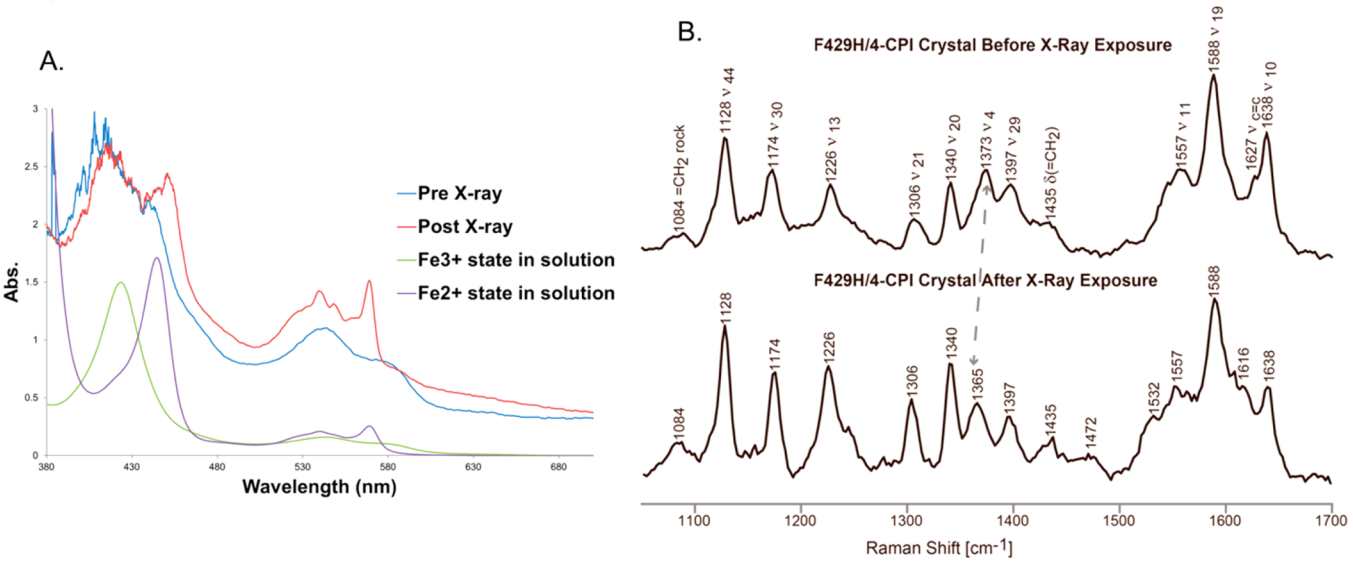

Figure 4. (A) UV–vis spectra from a single crystal of F429H/4-CPI before and following radiation. For comparison, the spectra of oxidized and reduced F429H/4-CPI in solution are presented. (B) High-frequency resonance Raman spectra recorded on a single crystal of F429H/4-CPI before and following exposure to X-rays. The oxidation-state marker band, ν_4, appearing at 1373 cm^{-1} for ferric F429H/4-CPI species before X-ray exposure was shifted down by 8 cm^{-1} to 1365 cm^{-1} following irradiation, indicating formation of ferrous F429H/4-CPI.

dx.doi.org/10.1021/bi5003794 | Biochemistry 2014, 53, 5080−5091

frequency, 1365 cm^{-1}, indicating the formation of the ferrous protein. In addition, the intensity of the "spin-state" marker band, ν_{10}, at 1638 cm^{-1} decreases upon irradiation of the crystal, consistent with partial reduction of the heme. To the best of our knowledge, this is the first demonstration of the reduction of a single crystal of a ferric microsomal P450 by both electronic and resonance Raman spectroscopy during the course of data collection.

Structure of 4-CPI-Bound CYP2B4 F429H. The 4-CPI-bound mutant protein F429H crystallized with a single molecule in the asymmetric unit. Table 4 provides the crystallographic data collection and refinement statistics. Its overall structure is a closed conformation similar to that of the 4-CPI-bound wild type protein [Protein Data Bank (PDB) entry 1SUO].[30]

Table 4. Crystallographic Data Collection and Refinement Statistics

	F429H/4-CPI
ligand	4-CPI
Data Collection	
beamline	BNL X29
wavelength (Å)	1.07500
space group	$P3_121$
cell dimensions	
a, *b*, *c* (Å)	91.492, 91.492, 150.380
α, *β*, *γ* (deg)	90, 90, 120
resolution range (Å)	79.2−2.4
no. of unique reflections	28505
completeness (high) (%)	97.7 (78.7)
redundancy	6.0 (5.7)
I/σ (high)	27.0 (3.4)
R_{merge} (high) (%)	6.1 (54.2)
Refinement	
resolution range (Å)	38.3−2.4
no. of reflections	28396
no. of reflections in test set	2860
R_{work}/R_{free} (%)	21.29/24.30
no. of molecules per asymmetric unit	1
no. of protein atoms	7268
no. of heteroatoms	198
no. of solvent atoms	106
average *B* factor (Å^2)	75.46
Ramachandran plot (%)	
preferred	97.1
allowed	2.9
outliers	0.0
rmsd for bond lengths (Å)	0.01
rmsd for bond angles (deg)	0.97

The conserved phenylalanine is the first residue in the conserved secondary structure known as the *β*-bulge, whereas the axial cysteine is the last residue (F429−C436) (Figure 5).[58] The rigid *β*-bulge (1) enforces close contact between the cysteine and its neighboring residues, (2) contains two residues, Arg434 and Ser430, that form a salt bridge and an H-bond with the D and A heme propionates, respectively, and (3) partially shields the heme from contact with solvent and solutes.

The most notable unique feature of the structure is the formation of a hydrogen bond between the *δ*N atom of His429 and the thiolate of axial cysteine 436 (Figure 6). The hydrogen−sulfur distance was 2.63 Å; the *δ*N−H···S angle

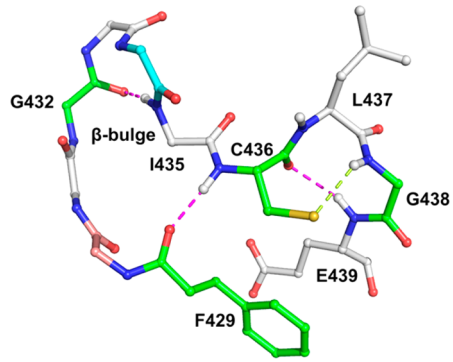

Figure 5. Structure of the *β*-bulge and *β*-turn of CYP2B4 (PDB entry 1SUO). Hydrogen bonds between the backbone and side chain of Cys436 and residues in the *β*-bulge preceding and the *β*-turn following the axial cysteine are illustrated. The backbone of the conserved residues is colored green. Note that the amide of Leu437 is pointing away from the thiolate. Residues Cys436−Glu439 form a typical *β*-turn that is characterized by a hydrogen bond between the carbonyl of the first residue (Cys436) and the amide of the fourth residue (Glu439). The first residue in such a turn is often a serine, threonine, or cysteine whose side chain forms a hydrogen bond with the amide of the third residue in the turn. The hydrogen bond between the thiolate and amide of Gly438 is colored light green. Side chains of residues Ser430−Ile435 are not shown for the sake of clarity.

was 145°. The introduced histidine replaces a phenylalanine whose aromatic ring *δ*H atom with a partial positive charge is in vdw contact with the thiolate and the heme.[59,60] The structure and biochemical data are consistent and demonstrate that the activity of P450s and electron density on the heme iron can be regulated by the entity interacting with the nonbonded lone electron pair on the thiolate. The experimental uncertainty of the Fe−S bond length in the crystal structure would not allow a firm conclusion with respect to its magnitude. However, it does explain the structural basis of the observation of a weaker Fe−S bond in the mutant by resonance Raman spectroscopy.[29]

Two additional differences were noted between the mutant and wild type. The *ε*N atom of the introduced histidine forms a hydrogen bond with a water molecule and also the amide side chain of Gln357 (Figure 6). The water molecule also hydrogen bonds to the carbonyl of the Gln357 side chain. For comparison, the more hydrophobic proximal surface of the corresponding P450 BM3 Phe393His mutant that lacks a histidine−thiolate bond[13] is shown (Figure 6).

Two factors likely contribute to thiolate H-bond formation in CYP2B4 F429H. The first is the more hydrophilic environment on the proximal surface of CYP2B4, which is able to stabilize the lone pair of electrons on the *ε*N atom of histidine by facilitating the formation of hydrogen bonds to the solvent and the side chain amide of Gln357 (Figure 6). If His393 assumes a conformation similar to that of His429 of CYP2B4, the lone pair of electrons on an *ε*N atom would encounter a hydrophobic cluster of four leucines that would discourage the formation of a hydrogen bond with the solvent. Although the *ε*N atom of His393 is not stabilized by water, the *δ*N atom of His393 forms a hydrogen bond to water. If H393 were protonated, the theoretical data in Table 7 indicate that it would exert a significant electron withdrawing effect on the axial thiolate. The second consideration that promotes thiolate−*δ*N His429 hydrogen bond formation is the more favorable position (closer and at a more advantageous H-bond

dx.doi.org/10.1021/bi5003794 | *Biochemistry* 2014, 53, 5080−5091

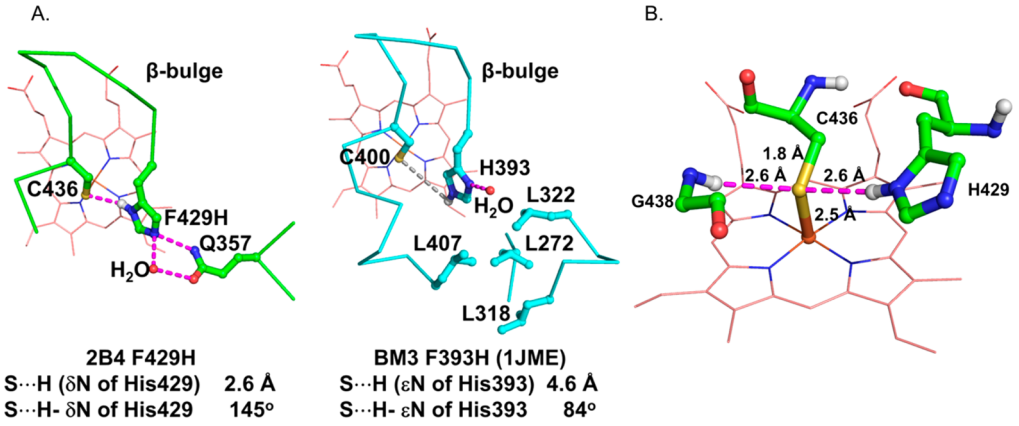

Figure 6. (A) Comparison of the histidine conformations and contacts on the proximal surface of F429H P450 2B4 and F393H P450 BM3 (PDB entry 1JME). Nitrogens are colored blue, hydrogens gray, and sulfurs yellow. Water is shown as a red sphere. Heme is shown with thin pink lines. In F429H, a hydrogen bond is formed between the δN atom of His429 and the thiolate of Cys436, whereas in F393H, a similar hydrogen bond is not present. The εN atom of His429 forms hydrogen bonds with water and the Gln357 side chain. (B) Tetrahedral configuration of Cys436 thiolate in F429H/4-CPI. Hydrogen bonds are shown between Cys436 and His429 and Gly438.

Table 5. Amide Hydrogen and Thiolate Bond Distances and N−H···S Angles for the Three Heme Pocket Residues C-Terminal to Cys (Cys-X1-Gly-X3)

			bond distance[a] (H···S) (Å)			angle (N−H···S) (deg)		
P450 (PDB entry)	P450 class	resolution (Å)	X1	G	X3	X1	G	X3
Fe^{3+} cam (2CPP)	I	1.63	3.7	2.5	3.2	73	129	91
11A1 (3N9Y)	I	2.1	3.6	2.6	3.1	73	123	89
2B4 (1SUO)	II	1.6	3.7	2.5	3.4	77	137	88
2B4 F429H/4-CPI	II	2.4	3.7	2.6	3.4	76	129	82
1A2 (2HI4)	II	1.95	3.5	2.3	3.2	76	147	89
102 μ_B3 (2J1M)	II	1.7	3.8	2.5	3.3	73	133	92
3A4 (3UA1)	II	2.15	3.9	2.8	3.4	75	128	83
176A1cin (4FMX)	II	1.55	3.6	2.6	3.4	77	136	87
152B1 SPα (3AWM)	III	1.65	Pro	2.3	3.8	Pro	146	93
74A AOS (2RCH)	III	1.85	3.7	2.5	3.6	75	140	85
8A1 (2B99)	III	2.50	Pro	2.6	3.3	Pro	133	102
55NOR (1JFB)	IV	1.0	3.6	2.6	3.5	81	140	87
mean ± standard deviation			3.7 ± 0.1	2.5 ± 0.1	3.3 ± 0.2	74 ± 3	137 ± 8	90 ± 6

[a]Hydrogen atoms were calculated in COOT.

Table 6. Thiolate Tetrahedral Angles (degrees)[a] Observed in P450s in Which the Second Lone Pair Forms an H-Bond

P450 (PDB entry)	Fe−S−Cβ	Fe−S−H (second lone pair)	Fe−S−H (Gly NH_2)	Cβ−S−H (second lone pair)	H (second lone pair)−S−H (Gly NH_2)	Cβ−S−H (Gly NH_2)
2B4 F429H/4CPI	103.04	**95.62**	96.12	**78.25**	**158.75**	116.02
102-BM3 F393A (1P0V)	104.63	**128.69**	108.97	**84.45**	**114.97**	109.85
	104.86[b]	**115.46**[b]	106.41[b]	**82.91**[b]	**131.38**[b]	109.74[b]
152A1 BSβ (1IZO)	106.46	**91.80**	117.28	**94.50**	**134.55**	108.06
152B1 SPα (3AWM)	107.00	**96.36**	117.41	**95.56**	**126.69**	110.54
NOS (1NSE)	110.34	**96.75**	110.76	**121.07**	**109.95**	107.50

[a]Angles involving the second lone pair are shown in bold. [b]Angle from the second molecule in the asymmetric unit, demonstrating range of angles in a protein. Hydrogens were generated in COOT.

angle) of a δN atom than an εN atom of imidazole with respect to the thiolate.

Nonbonded and Bonded Interactions of the Cys436 Thiolate. The cysteine thiolate in P450s possesses an sp^3 tetrahedral hybridization forming two covalent bonds, one with the heme iron and the other with the β-carbon of cysteine. One pair of the noncovalent bonded electrons forms an H-bond with the amide of the highly conserved Gly438 two residues to the carboxyl terminus of the axial thiolate. (Figures 5 and 6 and Table 5). In the wild type, the second nonbonded lone electron pair of the thiolate does not form a bond but is expected to occupy a region of high electron density extending toward the hydrogens on the aromatic ring of Phe429. The distance between the thiolate and the partially positively charged δH atom on the Phe429 aromatic ring (3 Å) is consistent with the lack of a formal hydrogen bond.[59,60] In the mutant, the weak interaction between the second, polarizable, nonbonded electron pair and the phenylalanine is replaced with a

dx.doi.org/10.1021/bi5003794 | Biochemistry 2014, 53, 5080−5091

histidine−thiolate hydrogen bond. Table 6 compares the tetrahedral angles observed in the F429H mutant and crystal structures of P450s and a nitric oxide synthase in which the nonbonded electron pair has formed a hydrogen bond with a fourth residue. Note that endothelial nitric oxide synthase, which lacks a P450 fold, has H-bonds between the thiolate and the glycine two residues to its C-terminus and the indole nitrogen of a tryptophan (Table 6).

In view of the tetrahedral nature of the thiolate, the properties of the putative additional hydrogen bonds between the thiolate and backbone amides of residues one (X1) and three (X3) residues to its C-terminus were examined (Table 5).[61,62] The H···S distance should be 0.2−0.5 Å shorter than the sum of the vdw radii of the hydrogen and sulfur atom (2.75 Å), and the N−H···S angle should deviate less than 25° from linear. There is more variability in the angles accepted for a hydrogen bond than in the distance between the atoms. Because the vdw radius of a sulfur atom with its large electron cloud is ∼0.4 Å greater than the radius of a nitrogen (1.55 Å) and an oxygen (1.52 Å), the S···H−X equilibrium length of a hydrogen bond between the sulfur and either a nitrogen or oxygen heteroatom will be ∼3.5 versus ∼3 Å for a hydrogen bond involving a heteroatom.[63,64]

Table 5, which was constructed using structures of class I−IV P450s determined to a resolution of 2.5 Å or better, indicates that in all four P450 classes only the conserved glycine, two residues downstream of the thiolates, forms a hydrogen bond with the thiolate in agreement with a previous study.[7,18] The amides of the first and third residues after the thiolate do not meet the criteria for hydrogen bond formation with the thiolate in either P450s or endothelial NOS. Mutation of the conserved glycine in the heme binding motif (FXXGXR/HXCXG) results in an inactive, unstable apoprotein, supporting a key role for this glycine in binding the heme and possibly also regulating the activity of P450s.[10] The instability of the glycine mutant severely limits an investigation of its exact role in catalysis (Figures 5 and 6). Identification of a single conserved hydrogen bond from a glycine two residues following the thiolate of P450s likely explains the anomalous mutagenesis results obtained in previous studies.[61,62]

Comparison of the Interaction Energy between the Cys436 Thiolate and His429 in Different Conformations and Protonation States. The total energy of interaction, E_{int}, between two objects is the sum of two terms: electrostatic (E_{elec}) and dispersion, that is, vdw (E_{disp}), forces. E_{elec} represents the energy due to electrostatic interactions of the point charges of the residue with the heme−thiolate moiety (see the Supporting Information for details of the theoretical calculations).The E_{disp} data in Table 7 provide the energetic contribution due to dispersion interactions (force between induced diploes) of residue 429 with the thiolate and with the heme ring due to an aromatic edge-to-face type interaction.[65,66] It is seen that E_{disp} is slightly larger for His429 than for Phe429. By contrast, the electrostatic interaction is much larger when Phe429 is replaced with a histidine whose δN atom can form a hydrogen bond with the thiolate. This interaction is further enhanced if the εN atom of His429 is protonated to form the positively charged imidazolium ion, which results in both a strong H-bond and a significant electrostatic interaction (E_{elec} = −28.8 kcal/mol) on the heme−thiolate moiety. To assess the role of the H-bond, we also rotated the imidazole ring by 180° around the β-carbon so that it cannot form an H-bond with the thiolate. As can be seen, the rotated doubly protonated positively charged His429 (HSP) resembles the His orientation in BM3 F393H and has an enhanced electrostatic interaction (E_{elec} = −22.9 kcal/mol) (Figure 6A), while the neutral single protonated state (HSD) loses its electrostatic interactions and experiences only weak vdw interactions with the heme unit (Figure 6A). The contribution of the interaction energy of Phe429 with the heme unit, including both the heme ring and thiolate, is predominantly a vdw interaction of an edge-to-face type as indicated in the dispersion energy column (E_{disp}) in Table 7.[65−67] By contrast, in F429H, His429 interacts with the heme−thiolate moiety by means of both vdw interactions and electrostatic interactions mainly resulting from the H-bonding of His429 to the thiolate ligand. The inhibitory effect of a histidine thiolate H-bond on P450 demonstrates that the thiolate lone pair is sensitive to electrostatic modulations and that phenylalanine plays an important role in protecting the thiolate lone pair from assuming undesired electrostatic interactions in P450s.

Table 7. Analysis of the Interaction Energies (E_{int}, in kilocalories per mole) of the Heme−Thiolate Moiety with Phe429 of the WT (Conf S)[a] and with His429 of the 4-CPI-Bound Mutant Structure in the Low-Spin Ferric State[b]

		E_{disp}		
residue 429	E_{elec}	E SH−Res	E Por−Res	E_{int}
Phe	−0.5	−1.1	−5.8	−7.4
HSD	−6.4	−1.3	−6.3	−13.9
His neutral				
HSP	−28.8	−2.1	−7.1	−38.0
His cationic				
HSD-180°, rotated	0.2	−0.5	−3.3	−3.6
His neutral				
HSP-180°, rotated	−22.9	−0.9	−5.2	−29.0
His cationic				

[a]QM/MM8 (quantum mechanics/molecular mechanics) optimized snapshot of a previous study (Figure S1 of the Supporting Information).[28] [b]The calculations were conducted using the UB3LYP/Def-TZVP level of theory.

The interactions of His with the heme−thiolate moiety are not constant and change somewhat along the catalytic cycle. Thus, the E_{int} in the ferric peroxo species of F429H reveals a stronger electrostatic interaction between the His and heme−thiolate moiety compared with that in the resting state [for HSD, neutral imidazole, and HSP, protonated positively charged imidazolium, E_{elec} = −16.7 and −140.3 kcal/mol, respectively (Table S1 of the Supporting Information)]. The His−thiolate interaction reduces the push effect of the thiolate and affects the various catalytic species. Thus, at various stations along the cycle, the F429H mutation engages in a variable interaction with the heme−thiolate moiety, which could affect the rate and thermodynamics of the step.[28,68] However, because the experimental results show that both the WT and the mutants give rise to formation of the hydroperoxo intermediate, very different activity must exist where O−O bond cleavage occurs.[27] Our recent theoretical calculations showed that the hydrogen bond donated by His429 to the thiolate reduces the electron density on the heme iron and impairs O−O bond cleavage and creates a tendency for homolytic bond O−O bond breaking instead of generating compound I by the heterolytic pathway.[28] By contrast, the effect of Phe429 is weak and the interaction with the heme−thiolate moiety does not impair the

dx.doi.org/10.1021/bi5003794 | Biochemistry 2014, 53, 5080−5091

Table 8. Characteristics of P450s Lacking the Conserved Phenylalanine

P450	Phe replacement	activity	active intermediate compound	other modifications: insert on proximal surface	other modifications: mutate I helix motif	surface charge modification vs P450 2B4	refs
CYP74A (AOS), allene oxide synthase	Trp	unsaturated fatty acid hydroperoxide alkyl dehydratase	II	+9 amino acids	yes	yes	21, 22
CYP74B (HPL), hydroperoxide lyase	Trp	unsaturated fatty acid alkyl hydroperoxide isomerase	II	+9 amino acids	yes	yes	21
CYP74D (DES), divinyl ether synthase	Trp	unsaturated fatty acid alkyl hydroperoxide dehydratase	II	+9 amino acids	yes	yes	21
CYP8A1, prostacyclin synthase	Trp	unsaturated fatty acid endoperoxide isomerase	II	+12 amino acids	yes	yes	23
CYP176A1 P450cin	Leu	monooxygenation of 1,8-cineole	I	no	yes	no	19
CYP152A1, P450 BSβ	Gln	fatty acid α and β C-hydroxylation	I	+4 amino acids	yes	yes	70
CYP152B1, P450 SPα	Gln	fatty acid α C-hydroxylation	I	+4 amino acids	yes	yes	69

electronic push effect of the thiolate in causing heterolytic O–O bond cleavage.

DISCUSSION

Comparison of the Structures of CYP2B4 F429H to Those of Class I and II P450s. To gain insight into the crucial role of Phe429 in P450 catalysis, we have compared the characteristics of the P450 F429H mutant to those of other mutant and wild type P450s lacking the conserved phenylalanine. The most thoroughly investigated homologous phenylalanine to histidine mutant (F393H) is from P450 BM3.[9,13−15] The F393H protein (1) has a 95 mV more positive redox potential and (2) is also reduced more quickly by the reductase. (3) However, it lacks an H-bond between the thiolate and the histidine. This is consistent with the EPR and resonance Raman spectra, which are similar to those of the wild type proteins. CYP2B4 F429H also has an 87 mV higher potential and is reduced more quickly by its reductase. However, an H-bond between the histidine and thiolate was observed crystallographically and was detected in the EPR and resonance Raman spectra of the F429H mutant.[13,15,27,29] Overall, the properties of the F429H mutant can be attributed to the electron withdrawing effect of the His–thiolate H-bond. In contrast, the structure of the heme domain of the BM3 F393H mutant would not fully account for all of the properties of the F393H mutant protein even if the histidine were protonated. However, a protonated cationic histidine (HSP) is not expected on the hydrophobic proximal surface of P450 BM3. In addition, an electron withdrawing effect on the heme iron strong enough to increase the potential, enhance heme reduction, stabilize the oxyferrous intermediate, and decrease activity would be expected to be reflected in the resonance Raman and EPR spectra. One possible explanation for the discrepancy is that the structure of the F393H mutant heme domain is different in the holoprotein.

The analogous F338H mutant of CYP121 is a notable exception to there being a critical role for the phenylalanine in redox potential modulation (PDB entry 1N40). It is atypical in that its redox properties are primarily controlled by the active site residue, Arg386.[20] Therefore, while the phenylalanine has been retained by CYP121, it no longer plays a critical role in the catalytic mechanism. $P450_{cin}$ is yet another variation. The phenylalanine is replaced with a leucine, yet the protein functions as a monooxygenase.[19] In $P450_{cam}$, the corresponding mutant, Phe350His, has not been crystallized and investigated to only a limited extent. The activity is decreased by ∼85%.[12]

Comparison of the Structures of CYP2B4 F429H to Those of Class III and IV P450s. There are three major categories of class III enzymes that employ oxygen-containing substrates or hydrogen peroxide but neither oxygen nor a redox partner. They are distinguished by the substrates they employ and the reactions they catalyze (summarized in Table 8). P450 SPα (CYP152B1) and BSβ (CYP152A1), in the first group, hydroxylate the carbon–hydrogen bonds of fatty acids presumably via a compound I intermediate by employing H_2O_2 and the salt bridge formed between the carboxylate of the substrate and an active site arginine.[69,70] (Table 8). The phenylalanine is replaced with glutamine, whose side chain amide forms a hydrogen bond with the axial thiolate. The likely explanation for compound I formation is a strong "pull" on electron density from the distal side of the heme as in peroxidases.

Allene oxide synthases (CYP74A), the second type of class III P450s, convert unsaturated fatty acid alkyl hydroperoxides into epoxides by dehydration, probably employing a compound II ($Fe^{4+}OH^-$) equivalent rather than compound I (Table 8). They are alkyl hydroperoxide dehydratases.[21,71] A tryptophan whose hydrogen on the aromatic ζ-carbon is in vdw contact with the thiolate replaces the conserved phenylalanine. On the distal side of the heme, the conserved I helix kink at the AGXET motif has shifted by three residues toward the N-terminus. An Asn side chain amide forms an H-bond with the iron-bound proximal oxygen of the substrate, which facilitates homolytic cleavage of the peroxide and formation of an epoxide (allene oxide) and water.

Prostacyclin synthase (CYP8A1) and thromboxane synthase (CYP5A1) are the third major type of class III P450s (Table 8). They both catalyze the isomerization, which proceeds via a Fe(IV)–porphyrin and alkoxy radical, of the same endoperoxide substrate, prostaglandin H_2, to two different epoxides that are key regulators of blood coagulation. The phenylalanine of prostacyclin synthase is replaced with a tryptophan whose benzene ring is in contact with the thiolate and heme.[23,72] The I helix AGXET sequence has mutated to ATQGN. Thromboxane synthase (CYP5A1), which, amazingly, is 57% similar to human CYP3A4, possesses the conserved phenylalanine,[72] and its conserved active site I helix motif has been retained except for the replacement of the conserved threonine with an isoleucine. The comparison made above illustrates that P450s

dx.doi.org/10.1021/bi5003794 | Biochemistry 2014, 53, 5080−5091

with drastically different sequences and, presumably, structures can nonetheless employ the identical substrate and catalyze a similar but distinct reaction.

Nitric oxide reductase (CYP 55, P450 NOR) is a class IV P450 that does not catalyze an oxidation; rather, it catalyzes the reduction of two molecules of nitric oxide (NO) to nitrous oxide (N_2O) and H_2O. NAD(P)H transfers a hydride ion directly to the nitric oxide-bound heme, a two-electron acceptor. Its heme pocket motif, including the conserved phenylalanine, has been preserved[24] (Table 8). The partially conserved active site I helix motif (AGNAT) stereospecifically binds NADPH but does not participate in proton delivery.

In summary, comparison of the mutant structure to structures of other P450s leads to the following conclusions. In class I and II P450s, the conserved phenylalanine is typically critical to the activity and thermodynamic properties of the protein while residues on the distal side of the heme are primarily involved in proton delivery and substrate binding. However, selected proteins (CYP121 and nitric oxide reductase) retain the phenylalanine but employ residues on the distal side of the heme to regulate the redox properties and the catalytic mechanism. The diverse class III P450s, typically alkyl hydroperoxide isomerases, often replace the phenylalanine with a tryptophan and redesign the distal heme pockets to perform the required plethora of biochemical transformations.

Notably, all four classes of P450s typically retain a conserved aromatic amino acid whose partially positive edge contacts both the thiolate where its nonbonded electron pair is predicted to occur and the partially negative face of the heme in an edge-to-face conformation. In this position, it is expected to protect the thiolate lone pair and the heme from side reactions, such as H-bond formation, with chemical entities and solvent. Additional functions (inhibition of oxidation and protonation of cysteine) of the phenylalanine and heme binding motif can be inferred from studies that have introduced a thiolate into a different proximal surface scaffold. Replacing the axial histidine of cyt *c* peroxidase, heme oxygenase, and myoglobin with cysteine resulted in oxidation of the cysteine to cysteic acid in cyt *c* peroxidase, while the cysteine in heme oxygenase and myoglobin became protonated and did not bind the ferrous heme as a result of exposure to bulk solvent.[73−75] Significant monooxygenase activity was not observed in any of the histidine to cysteine mutants. Understanding how P450s employ diverse, finely tuned protein environments to mediate their catalytic activities will aid scientists in designing novel pharmaceuticals and creating enzymes that can extend the chemical repertoire of natural P450s.

■ ASSOCIATED CONTENT

Supporting Information

Detailed information about construct design, expression, purification, and crystallization of truncated F429H/4-CPI; QM/MM setup and methodology; one figure, with key geometries of different states in QM/MM calculations; one table of energy analysis and QM coordinates; and references. This material is available free of charge via the Internet at http://pubs.acs.org.

Accession Codes

Data deposited as Protein Data Bank entry 4MGJ.

■ AUTHOR INFORMATION

Corresponding Author

*E-mail: waskell@umich.edu. Phone: (734) 845-5858.

Funding

This work was supported by National Institutes of Health Grants R01GM035533 and R01GM094209 and a VA Merit Review Grant to L.W.

Notes

The authors declare no competing financial interest.

■ ACKNOWLEDGMENTS

Use of PXRR beamlines X26C and X29 at the National Synchrotron Light Source was supported by the U.S. Department of Energy (DOE), Office of Basic Energy Sciences (DE-AC02-98CH10886). Use of the Advanced Photon Source was supported by the DOE (DE-AC02-06CH11357). Use of LS-CAT Sector 21 was supported by the Michigan Economic Development Corp. and the Michigan Technology Tri-Corridor (Grant 085P1000817). The excellent expert assistance of the staff at both synchrotrons is very much appreciated. Drs. Allen Orville, Deborah Stoner-Ma, and Grace Shea-McCarthy made possible collection of the UV−visible and resonance Raman spectra. Dr. David Smith of LS-CAT helped with remote data collection. We are grateful for the use of the X-ray facility at the Center for Structural Biology, Life Sciences Institute, University of Michigan. Dr. James Kincaid assisted with interpretation of the resonance Raman spectra.

■ ABBREVIATIONS

P450, cytochrome P450; CYP2B4, cytochrome P450 2B4; cyt b_5, cytochrome b_5; BHT, 2,6-di-*tert*-butyl-4-methylphenol; BP, benzphetamine; 4-CPI, 4-(4-chlorophenyl)imidazole; HSP, cationic protonated histidine; HSD, neutral histidine; QM/MM, quantum mechanics/molecular mechanics; rmsd, root-mean-square deviation; vdw, van der Waals.

■ REFERENCES

(1) Ortiz de Montellano, P. (2005) *Cytochrome P450: Structure, Mechanism, and Biochemistry*, 3rd ed., Kluwer Academic/Plenum Publishers, New York.

(2) Guengerich, F. P., and Munro, A. W. (2013) Unusual cytochrome P450 enzymes and reactions. *J. Biol. Chem. 288*, 17065−17073.

(3) Domanski, T. L., and Halpert, J. R. (2001) Analysis of mammalian cytochrome P450 structure and function by site-directed mutagenesis. *Curr. Drug Metab. 2*, 117−137.

(4) Johnson, E. F. (2003) The 2002 Bernard B. Brodie Award lecture: Deciphering substrate recognition by drug-metabolizing cytochromes P450. *Drug Metab. Dispos. 31*, 1532−1540.

(5) Guengerich, F. P. (2005) Human cytochrome P450 Enzymes. In *Cytochrome P450: Structure, Mechanism, and Biochemistry* (Ortiz de Montellano, P., Ed.) 3rd ed., pp 377−530, Kluwer Academic/Plenum Publishers, New York.

(6) Shen, A. L., O'Leary, K. A., and Kasper, C. B. (2002) Association of multiple developmental defects and embryonic lethality with loss of microsomal NADPH-cytochrome P450 oxidoreductase. *J. Biol. Chem. 277*, 6536−6541.

(7) Mestres, J. (2005) Structure conservation in cytochromes P450. *Proteins 58*, 596−609.

(8) Nelson, D. R. (2009) The cytochrome P450 homepage. *Hum. Genomics 4*, 59−65.

(9) Ost, T. W., Miles, C. S., Munro, A. W., Murdoch, J., Reid, G. A., and Chapman, S. K. (2001) Phenylalanine 393 exerts thermodynamic control over the heme of flavocytochrome P450 BM3. *Biochemistry 40*, 13421−13429.

(10) Shimizu, T., Hirano, K., Takahashi, M., Hatano, M., and Fujii-Kuriyama, Y. (1988) Site-directed mutageneses of rat liver cytochrome P-450d: Axial ligand and heme incorporation. *Biochemistry 27*, 4138–4141.
(11) Porter, T. D. (1994) Mutagenesis at a highly conserved phenylalanine in cytochrome P450 2E1 affects heme incorporation and catalytic activity. *Biochemistry 33*, 5942–5946.
(12) Yasukochi, T., Okada, O., Hara, T., Sagara, Y., Sekimizu, K., and Horiuchi, T. (1994) Putative functions of phenylalanine-350 of *Pseudomonas putida* cytochrome P-450cam. *Biochim. Biophys. Acta 1204*, 84–90.
(13) Ost, T. W., Munro, A. W., Mowat, C. G., Taylor, P. R., Pesseguiero, A., Fulco, A. J., Cho, A. K., Cheesman, M. A., Walkinshaw, M. D., and Chapman, S. K. (2001) Structural and spectroscopic analysis of the F393H mutant of flavocytochrome P450 BM3. *Biochemistry 40*, 13430–13438.
(14) Ost, T. W., Clark, J., Mowat, C. G., Miles, C. S., Walkinshaw, M. D., Reid, G. A., Chapman, S. K., and Daff, S. (2003) Oxygen activation and electron transfer in flavocytochrome P450 BM3. *J. Am. Chem. Soc. 125*, 15010–15020.
(15) Chen, Z., Ost, T. W., and Schelvis, J. P. (2004) Phe393 mutants of cytochrome P450 BM3 with modified heme redox potentials have altered heme vinyl and propionate conformations. *Biochemistry 43*, 1798–1808.
(16) Matsumura, H., Wakatabi, M., Omi, S., Ohtaki, A., Nakamura, N., Yohda, M., and Ohno, H. (2008) Modulation of redox potential and alteration in reactivity via the peroxide shunt pathway by mutation of cytochrome P450 around the proximal heme ligand. *Biochemistry 47*, 4834–4842.
(17) Quaroni, L. G., Seward, H. E., McLean, K. J., Girvan, H. M., Ost, T. W., Noble, M. A., Kelly, S. M., Price, N. C., Cheesman, M. R., Smith, W. E., and Munro, A. W. (2004) Interaction of nitric oxide with cytochrome P450 BM3. *Biochemistry 43*, 16416–16431.
(18) Meharenna, Y. T., Li, H., Hawkes, D. B., Pearson, A. G., De Voss, J., and Poulos, T. L. (2004) Crystal structure of P450cin in a complex with its substrate, 1,8-cineole, a close structural homologue to D-camphor, the substrate for P450cam. *Biochemistry 43*, 9487–9494.
(19) Madronaqq, Y., Tripathi, S., Li, H., and Poulos, T. L. (2012) Crystal structures of substrate-free and nitrosyl cytochrome P450cin: Implications for O_2 activation. *Biochemistry 51*, 6623–6631.
(20) McLean, K. J., Carroll, P., Lewis, D. G., Dunford, A. J., Seward, H. E., Neeli, R., Cheesman, M. R., Marsollier, L., Douglas, P., Smith, W. E., Rosenkrands, I., Cole, S. T., Leys, D., Parish, T., and Munro, A. W. (2008) Characterization of active site structure in CYP121. A cytochrome P450 essential for viability of *Mycobacterium tuberculosis* H37Rv. *J. Biol. Chem. 283*, 33406–33416.
(21) Lee, D. S., Nioche, P., Hamberg, M., and Raman, C. S. (2008) Structural insights into the evolutionary paths of oxylipin biosynthetic enzymes. *Nature 455*, 363–368.
(22) Li, L., Chang, Z., Pan, Z., Fu, Z. Q., and Wang, X. (2008) Modes of heme binding and substrate access for cytochrome P450 CYP74A revealed by crystal structures of allene oxide synthase. *Proc. Natl. Acad. Sci. U.S.A. 105*, 13883–13888.
(23) Li, Y. C., Chiang, C. W., Yeh, H. C., Hsu, P. Y., Whitby, F. G., Wang, L. H., and Chan, N. L. (2008) Structures of prostacyclin synthase and its complexes with substrate analog and inhibitor reveal a ligand-specific heme conformation change. *J. Biol. Chem. 283*, 2917–2926.
(24) Park, S. Y., Shimizu, H., Adachi, S., Nakagawa, A., Tanaka, I., Nakahara, K., Shoun, H., Obayashi, E., Nakamura, H., Iizuka, T., and Shiro, Y. (1997) Crystal structure of nitric oxide reductase from denitrifying fungus *Fusarium oxysporum*. *Nat. Struct. Biol. 4*, 827–832.
(25) Aldag, C., Gromov, I. A., Garcia-Rubio, I., von Koenig, K., Schlichting, I., Jaun, B., and Hilvert, D. (2009) Probing the role of the proximal heme ligand in cytochrome P450cam by recombinant incorporation of selenocysteine. *Proc. Natl. Acad. Sci. U.S.A. 106*, 5481–5486.
(26) Perera, R., Sono, M., Kinloch, R., Zhang, H., Tarasev, M., Im, S. C., Waskell, L., and Dawson, J. H. (2011) Stabilization and spectroscopic characterization of the dioxygen complex of wild-type cytochrome P4502B4 (CYP2B4) and its distal side E301Q, T302A and proximal side F429H mutants at subzero temperatures. *Biochim. Biophys. Acta 1814*, 69–75.
(27) Davydov, R., Razeghifard, R., Im, S. C., Waskell, L., and Hoffman, B. M. (2008) Characterization of the microsomal cytochrome P450 2B4 O_2 activation intermediates by cryoreduction and electron paramagnetic resonance. *Biochemistry 47*, 9661–9666.
(28) Usharani, D., Zazza, C., Lai, W., Chourasia, M., Waskell, L., and Shaik, S. (2012) A single-site mutation (F429H) converts the enzyme CYP 2B4 into a heme oxygenase: A QM/MM study. *J. Am. Chem. Soc. 134*, 4053–4056.
(29) Mak, P. J., Yang, Y., Im, S., Waskell, L. A., and Kincaid, J. R. (2012) Experimental documentation of the structural consequences of hydrogen-bonding interactions to the proximal cysteine of a cytochrome P450. *Angew. Chem., Int. Ed. 51*, 10403–10407.
(30) Scott, E. E., White, M. A., He, Y. A., Johnson, E. F., Stout, C. D., and Halpert, J. R. (2004) Structure of mammalian cytochrome P450 2B4 complexed with 4-(4-chlorophenyl)imidazole at 1.9-Å resolution: Insight into the range of P450 conformations and the coordination of redox partner binding. *J. Biol. Chem. 279*, 27294–27301.
(31) Saribas, A. S., Gruenke, L., and Waskell, L. (2001) Over-expression and purification of the membrane-bound cytochrome P450 2B4. *Protein Expression Purif. 21*, 303–309.
(32) Otwinowski, Z., and Minor, W. (1997) Processing of X-ray diffraction data collected in oscillation mode. In *Macromolecular Crystallography, Part A* (Carter, C. W. J., and Sweet, R. M., Eds.) pp 307–326, Academic Press, New York.
(33) McCoy, A. J., Grosse-Kunstleve, R. W., Adams, P. D., Winn, M. D., Storoni, L. C., and Read, R. J. (2007) Phaser crystallographic software. *J. Appl. Crystallogr. 40*, 658–674.
(34) Winn, M. D., Ballard, C. C., Cowtan, K. D., Dodson, E. J., Emsley, P., Evans, P. R., Keegan, R. M., Krissinel, E. B., Leslie, A. G., McCoy, A., McNicholas, S. J., Murshudov, G. N., Pannu, N. S., Potterton, E. A., Powell, H. R., Read, R. J., Vagin, A., and Wilson, K. S. (2011) Overview of the CCP4 suite and current developments. *Acta Crystallogr. D67*, 235–242.
(35) Bricogne, G., Blanc, E., Brandl, M., Flensburg, C., Keller, P., Paciorek, W., Roversi, P., Sharff, A., Smart, O. S., Vonrhein, C., and Womack, T. O. (2011) *BUSTER*, version 2.10.0, Global Phasing Ltd., Cambridge, U.K.
(36) Emsley, P., Lohkamp, B., Scott, W. G., and Cowtan, K. (2010) Features and development of Coot. *Acta Crystallogr. D66*, 486–501.
(37) Kleywegt, G. J. (2007) Quality control and validation. *Methods Mol. Biol. 364*, 255–272.
(38) Smart, O. S., Womack, T. O., Sharff, A., Flensburg, C., Keller, P., Paciorek, W., Vonrhein, C., and Bricogne, G. (2011) *Grade*, version 1.1.1, Global Phasing Ltd., Cambridge, U.K.
(39) Davis, I. W., Leaver-Fay, A., Chen, V. B., Block, J. N., Kapral, G. J., Wang, X., Murray, L. W., Arendall, W. B., III, Snoeyink, J., Richardson, J. S., and Richardson, D. C. (2007) MolProbity: All-atom contacts and structure validation for proteins and nucleic acids. *Nucleic Acids Res. 35*, W375–W383.
(40) Bridges, A., Gruenke, L., Chang, Y. T., Vakser, I. A., Loew, G., and Waskell, L. (1998) Identification of the binding site on cytochrome P450 2B4 for cytochrome b5 and cytochrome P450 reductase. *J. Biol. Chem. 273*, 17036–17049.
(41) Hamdane, D., Xia, C., Im, S. C., Zhang, H., Kim, J. J., and Waskell, L. (2009) Structure and function of an NADPH-cytochrome P450 oxidoreductase in an open conformation capable of reducing cytochrome P450. *J. Biol. Chem. 284*, 11374–11384.
(42) Jefcoate, C. R. (1978) Measurement of substrate and inhibitor binding to microsomal cytochrome P-450 by optical-difference spectroscopy. *Methods Enzymol. 52*, 258–279.
(43) Guengerich, F. P., Ballou, D. P., and Coon, M. J. (1975) Purified liver microsomal cytochrome P-450. Electron-accepting properties and oxidation-reduction potential. *J. Biol. Chem. 250*, 7405–7414.

(44) Heo, J., Halbleib, C. M., and Ludden, P. W. (2001) Redox-dependent activation of CO dehydrogenase from *Rhodospirillum rubrum*. *Proc. Natl. Acad. Sci. U.S.A. 98*, 7690−7693.
(45) Oprian, D. D., Vatsis, K. P., and Coon, M. J. (1979) Kinetics of reduction of cytochrome P-450LM4 in a reconstituted liver microsomal enzyme system. *J. Biol. Chem. 254*, 8895−8902.
(46) Gray, R. D. (1982) Kinetics and Mechanism of Carbon-Monoxide Binding to Purified Liver Microsomal Cytochrome-P-450 Isozymes. *J. Biol. Chem. 257*, 1086−1094.
(47) Zhang, H., Gruenke, L., Arscott, D., Shen, A., Kasper, C., Harris, D. L., Glavanovich, M., Johnson, R., and Waskell, L. (2003) Determination of the rate of reduction of oxyferrous cytochrome P450 2B4 by 5-deazariboflavin adenine dinucleotide T491V cytochrome P450 reductase. *Biochemistry 42*, 11594−11603.
(48) Hanson, L. K., Eaton, W. A., Sligar, S. G., Gunsalus, I. C., Gouterman, M., and Connell, C. R. (1976) Letter: Origin of the anomalous Soret spectra of carboxycytochrome P-450. *J. Am. Chem. Soc. 98*, 2672−2674.
(49) Sivaramakrishnan, S., Ouellet, H., Matsumura, H., Guan, S., Moenne-Loccoz, P., Burlingame, A. L., and Ortiz de Montellano, P. R. (2012) Proximal ligand electron donation and reactivity of the cytochrome P450 ferric-peroxo anion. *J. Am. Chem. Soc. 134*, 6673−6684.
(50) Bonfils, C., Balny, C., and Maurel, P. (1981) Direct evidence for electron transfer from ferrous cytochrome b5 to the oxyferrous intermediate of liver microsomal cytochrome P-450 LM2. *J. Biol. Chem. 256*, 9457−9465.
(51) Ogliaro, F., de Visser, S. P., and Shaik, S. (2002) The 'push' effect of the thiolate ligand in cytochrome P450: A theoretical gauging. *J. Inorg. Biochem. 91*, 554−567.
(52) Ueyama, N., Nishikawa, N., Yamada, Y., Okamura, T., and Nakamura, A. (1996) Cytochrome P-450 model (porphinato)-(thiolato)iron(III) complexes with single and double NH···S hydrogen bonds at the thiolate site. *J. Am. Chem. Soc. 118*, 12826−12827.
(53) Beitlich, T., Kuhnel, K., Schulze-Briese, C., Shoeman, R. L., and Schlichting, I. (2007) Cryoradiolytic reduction of crystalline heme proteins: Analysis by UV-vis spectroscopy and X-ray crystallography. *J. Synchrotron Radiat. 14*, 11−23.
(54) Kuhnel, K., Derat, E., Terner, J., Shaik, S., and Schlichting, I. (2007) Structure and quantum chemical characterization of chloroperoxidase compound 0, a common reaction intermediate of diverse heme enzymes. *Proc. Natl. Acad. Sci. U.S.A. 104*, 99−104.
(55) Schlichting, I., Berendzen, J., Chu, K., Stock, A. M., Maves, S. A., Benson, D. E., Sweet, R. M., Ringe, D., Petsko, G. A., and Sligar, S. G. (2000) The catalytic pathway of cytochrome p450cam at atomic resolution. *Science 287*, 1615−1622.
(56) De la Mora, E., Lovett, J. E., Blanford, C. F., Garman, E. F., Valderrama, B., and Rudino-Pinera, E. (2012) Structural changes caused by radiation-induced reduction and radiolysis: The effect of X-ray absorbed dose in a fungal multicopper oxidase. *Acta Crystallogr. D68*, 564−577.
(57) Garman, E. F. (2010) Radiation damage in macromolecular crystallography: What is it and why should we care? *Acta Crystallogr. D66*, 339−351.
(58) Richardson, J. S., Getzoff, E. D., and Richardson, D. C. (1978) β-Bulge: Common Small Unit of Nonrepetitive Protein-Structure. *Proc. Natl. Acad. Sci. U.S.A. 75*, 2574−2578.
(59) Dougherty, D. A. (1996) Cation-π interactions in chemistry and biology: A new view of benzene, Phe, Tyr, and Trp. *Science 271*, 163−168.
(60) Mecozzi, S., West, A. P., Jr., and Dougherty, D. A. (1996) Cation-π interactions in aromatics of biological and medicinal interest: Electrostatic potential surfaces as a useful qualitative guide. *Proc. Natl. Acad. Sci. U.S.A. 93*, 10566−10571.
(61) Yoshioka, S., Tosha, T., Takahashi, S., Ishimori, K., Hori, H., and Morishima, I. (2002) Roles of the proximal hydrogen bonding network in cytochrome P450cam-catalyzed oxygenation. *J. Am. Chem. Soc. 124*, 14571−14579.
(62) Galinato, M. G., Spolitak, T., Ballou, D. P., and Lehnert, N. (2011) Elucidating the role of the proximal cysteine hydrogen-bonding network in ferric cytochrome P450cam and corresponding mutants using magnetic circular dichroism spectroscopy. *Biochemistry 50*, 1053−1069.
(63) Gregoret, L. M., Rader, S. D., Fletterick, R. J., and Cohen, F. E. (1991) Hydrogen bonds involving sulfur atoms in proteins. *Proteins 9*, 99−107.
(64) Donohue, J. (1969) On N-H–S hydrogen bonds. *J. Mol. Biol. 45*, 231−235.
(65) Burley, S. K., and Petsko, G. A. (1985) Aromatic-aromatic interaction: A mechanism of protein structure stabilization. *Science 229*, 23−28.
(66) Martinez, C. R., and Iverson, B. L. (2012) Rethinking the term "π-stacking". *Chem. Sci. 3*, 2191−2201.
(67) Grimme, S., Antony, J., Ehrlich, S., and Krieg, H. (2010) A consistent and accurate ab initio parametrization of density functional dispersion correction (DFT-D) for the 94 elements H-Pu. *J. Chem. Phys. 132*, 154104.
(68) Dawson, J. H. (1988) Probing structure-function relations in heme-containing oxygenases and peroxidases. *Science 240*, 433−439.
(69) Fujishiro, T., Shoji, O., Nagano, S., Sugimoto, H., Shiro, Y., and Watanabe, Y. (2011) Crystal structure of H_2O_2-dependent cytochrome P450SPα with its bound fatty acid substrate: Insight into the regioselective hydroxylation of fatty acids at the α position. *J. Biol. Chem. 286*, 29941−29950.
(70) Shoji, O., Fujishiro, T., Nagano, S., Tanaka, S., Hirose, T., Shiro, Y., and Watanabe, Y. (2010) Understanding substrate misrecognition of hydrogen peroxide dependent cytochrome P450 from *Bacillus subtilis*. *J. Biol. Inorg. Chem. 15*, 1331−1339.
(71) Brash, A. R. (2009) Mechanistic aspects of CYP74 allene oxide synthases and related cytochrome P450 enzymes. *Phytochemistry 70*, 1522−1531.
(72) Sirim, D., Widmann, M., Wagner, F., and Pleiss, J. (2010) Prediction and analysis of the modular structure of cytochrome P450 monooxygenases. *BMC Struct. Biol. 10*, 34.
(73) Choudhury, K., Sundaramoorthy, M., Hickman, A., Yonetani, T., Woehl, E., Dunn, M. F., and Poulos, T. L. (1994) Role of the proximal ligand in peroxidase catalysis. Crystallographic, kinetic, and spectral studies of cytochrome c peroxidase proximal ligand mutants. *J. Biol. Chem. 269*, 20239−20249.
(74) Liu, Y., Moeenee-Loccoz, P., Hildebrand, D. P., Wilks, A., Hoehr, T. M., Mauk, A. G., and Ortiz de Montellano, P. R. (1999) Replacement of the proximal histidine iron ligand by a cysteine or tyrosine converts heme oxygenase to an oxidase. *Biochemistry 38*, 3733−3743.
(75) Adachi, S., Nagano, S., Ishimori, K., Watanabe, Y., Morishima, I., Egawa, T., Kitagawa, T., and Makino, R. (1993) Roles of proximal ligand in heme proteins: Replacement of proximal histidine of human myoglobin with cysteine and tyrosine by site-directed mutagenesis as models for P-450, chloroperoxidase, and catalase. *Biochemistry 32*, 241−252.